

Article

The Effect of Rice Straw Gasification Temperature on the Release and Occurrence Modes of Na and K in a Fluidized Bed

Tianyu Chen, Jun Cao and Baosheng Jin *

Key Laboratory of Energy Thermal Conversion and Control of Ministry of Education,
School of Energy and Environment, Southeast University, Nanjing 210096, China;
chentianyu8968@outlook.com (T.C.); caojunxm@126.com (J.C.)

* Correspondence: bsjin@seu.edu.cn; Tel.: +86-25-83792506; Fax: +86-25-83795508

Received: 12 September 2017; Accepted: 20 November 2017; Published: 23 November 2017

Abstract: Rice straw gasification was carried out in a laboratory fluidized bed reactor system from 600 to 800 °C in order to well-understand the release and occurrence mode of alkali metals as a function of temperature during the gasification process. Inductively coupled plasma atomic emission spectrometry (ICP-AES) was applied to analyze the original rice straw and obtained fly ash at different temperatures. The results show that the Water-Soluble, Ammonium acetate-Soluble, Hydrochloric acid-Soluble, and Aluminosilicate Combination-Soluble modes of the Na and K contents in rice straw decreased in sequence. The content of Water-Soluble salts of Na and K accounts for more than 50%, while the content of the Aluminosilicate Combination-Soluble mode is the lowest: less than 5%. The release rate of Na appears to be consistent but nonlinear, increasing with gasification conversion ranges between 50.2% and 70.8%, from which we can deduce that temperature is not the only factor that impacts Na emission. The release of K can be divided into two stages at 700 °C. At the first stage, the release rate of K is almost invariable, ranging from 23.3% to 26%. At the second stage, the release rate increases sharply: up to 55.9%. The concentration and the proportion of the Water-Soluble, Ammonium acetate-Soluble, and Hydrochloric acid-Soluble modes of Na in fly ash decrease with a temperature increase. The release of K can be explained as follows: one path is an organic form of K converted into its gaseous phase; the other path is a soluble inorganic form of K that is volatile at a high temperature. With a temperature increase, the Aluminosilicate Combination-Soluble mode of both Na and K increases.

Keywords: rice straw; gasification; alkali metals; occurrence mode

1. Introduction

Besides solar and wind energy, biomass is considered to be a main renewable energy source, which can be used as adjustable, controlled energy in a renewable energy mixture of solar, wind, and biomass energy. The utilization of biomass is an effective solution for global warming and climate change. Unlike fossil fuels production, there are far less geographical restrictions for biomass production in most non-desert countries, so biomass utilization is also an important part of national energy security for non-OPEC (non-Organization of Petroleum Exporting Countries) countries. In recent decades, the energy supply derived from biomass keeps growing, while that from wind and solar is still at a low level [1].

As a key technology for biomass utilization, biomass gasification represents an efficient process for the production of power and heat and the production of hydrogen and second-generation biofuels. Gasification can theoretically convert all different types of biomass into syngas, which is mainly composed of hydrogen, carbon monoxide, carbon dioxide, and methane, for use as gas fuel and raw

material for hydrogen production and other chemical productions [2,3]. Unlike most fossil fuels, natural biomass is highly enriched in potassium (K), sodium (Na), and chlorine (Cl), especially when it derives from agricultural residues such as straw [4,5]. During the thermal treatment of biomass in a gasifier, the alkali metals release to the gas phase and subsequently cause slagging, agglomeration, deposition, and corrosion in thermal fuel conversion systems [6–13]. These problems seriously affect the safety of reactors' operation and reduce their thermal efficiency. However, on the other hand, the alkali metals play a catalytic role in the thermal utilization process, resulting in a rate increase of biomass decomposition, a yield increase of gas and char, and a yield decrease of tar [14]. During the gasification process, the alkali metals' residues on the char result in a decrease of the gasification temperature, an improvement in gasification efficiency, and a change in the products' composition [15–17]. Bouraoui et al. [18,19] studied the effects of K and Si as mineral contents and the textural and structural properties of biomass on the CO₂ gasification reactivity of a biomass char using a thermogravimetric analysis. The results showed that when the conversion rate reaches 60%, the presence of K and Si becomes the major parameter influencing reactivity. Therefore, a good understanding of alkali metals' migration and transformation during the gasification process is highly significant for the resourceful utilization of biomass.

There has been much research on the release of alkali metals during the biomass thermal treatment process. Joakim et al. [20] studied the release of critical ash-forming elements from the combustion of biomass containing K, Cl, and S. Keown et al. [21] conducted a pyrolysis of sugar cane bagasse and cane trash in a quartz fluidized-bed reactor, and found that less than 20% of the alkali metals volatilized from biomass samples at a slow heating rate (10 K/min), while 80% of the alkali metals volatilized at fast heating rates (>1000 K/s). There are four kinds of occurrence forms of alkali metals in biomass. The first one is the Water-Soluble form, in which alkali metals exist as ions and are soluble in water, ammonium acetate, and hydrochloric acid. The second one is the Ammonium acetate-Soluble form, in which alkali metals exist as carboxylate and coordination forms in nitrogen and oxygen functional groups. Ammonium acetate-Soluble alkali metals are insoluble in water, but are soluble in ammonium acetate and hydrochloric acid. The third one is the Hydrochloric acid-Soluble form, in which alkali metals attach to the ash surface in a non-crystalline form and are insoluble in ammonium acetate but soluble in hydrochloric acid. The last one is the Aluminosilicate Combination-Soluble form, in which alkali metals are insoluble in water, ammonium acetate, and hydrochloric acid. Generally, the first three forms are usually easy to evaporate while the last is difficult.

The total amount of changes of alkali metals released during the thermal treatment process has been reported a lot by previous research, but the changes of alkali metals' forms, especially K's and Na's forms, have not been paid sufficient attention [22,23]. If we can grasp the form change of alkali metals, then the behaviors of slagging, agglomeration, deposition, corrosion, and catalysis could be understood better.

The objective of this paper is to obtain the release and transformation regularities of the occurrence forms of K and Na during the gasification process. The experiments were carried out by using a laboratory fluidized bed reactor. Rice straw was used as the raw material for biomass gasification. The gasification temperature ranged from 600 to 800 °C with 50 °C increments. The results in this paper could provide theoretical bases for the large-scale application of biomass gasification in the future.

2. Experimental

2.1. Biomass

The rice straw used in this experiment was collected from a rural area in Jiangsu Province, China. Robust and healthy rice straw with a uniform particle size and density, 0.5–2 mm and 379 kg/m³, respectively, was selected to ensure accurate measurements. The rice straw was firstly dried in air, then pressed, and finally dried under 105 °C for 3 h in an oven. The proximate analysis and the elemental analysis of the rice straw are listed in Table 1. The ash was obtained through raw sample

oxidization in a low-temperature asher (K1050X, EMITECH Company, East Sussex, UK), which caused almost no evaporation of inorganic mineral, and then was analyzed by an X-ray fluorescence probe (ARL, Thermal Company, Madison, AL, USA). The residual after the treatment by the low-temperature asher will be abbreviated as “LTA” hereafter. The composition of the LTA is shown in Table 2.

Table 1. Proximate analysis and elemental analysis ¹.

Proximate Analysis (wt %, daf)				Elemental Analysis (wt %, ad)					Weight Ratios	
M _{ad}	V _{daf}	FC _d	A _d	C _{daf}	H _{daf}	N _{daf}	O _{daf}	S _d	H/C ratio	O/C ratio
3.58	76.28	14.8	5.34	51.67	6.21	1.44	40.45	0.2	0.120	0.783

¹ daf: dry ash-free basis; ad: as air dried basis; d: dried basis; M: moisture, V: volatile matter, FC: fixed carbon, A: ash.

Table 2. The ash content of rice straw.

Content	Na ₂ O	K ₂ O	SO ₃	MnO	Al ₂ O ₃	P ₂ O ₅	CaO	MgO	SiO ₂	Fe ₂ O ₃	Others
%	2.43	7.52	0.58	0.14	1.20	4.02	2.44	3.18	73.65	0.16	4.68

Compared with industrial by product and agro-industrial and marine biomass in the literature [24], the rice straw as an agricultural residue shows higher amounts of volatiles—more than 70%—but relatively lower ash contents. The high amount of volatile matter in the original rice straw as shown in Table 1 means the fuels mainly content lignin, cellulose, and hemicellulose [25]. The total amount of the content of LTA is as low as 5.34%. Additionally, SiO₂ plays an important role in the LTA, about 73.65%, while alkali metals account for 9.95%.

Each test was performed in identical conditions to guarantee the accuracy of the experimental results, and the margin of error between replicated experiments was maintained below 3%.

2.2. Experimental Method

The alkali metal transformation mechanism was conducted in a biomass gasification fluidized bed experiment system as shown in Figure 1. The system setup was mainly composed of five units: a gas applying unit, a fuel applying unit, a fluidized bed reactor, a gas purifying unit, and a gas sampling and discharging unit. The fuels were continuously fed in the reactor at 1.11 kg/h by a screw feeder. The fluidized bed reactor was made of 2520 stainless with an inner diameter of 50 mm and a length of 1200 mm. The bottom of the bed uses a hood-type distributor to ensure that the air is well-distributed. The reactor was externally heated by a resistance furnace controlled by a Proportion-Integral-Derivative (PID) temperature programmed controller. Two alumel/chromel thermocouples were placed inside the tube to monitor the temperatures of the dense phase and the dilute phase, respectively, represented by red color. In order to prevent the fuel coking, a certain amount of hot air was carried to the reactor. When the temperature was up to a set point (600, 650, 700, 750 and 800 °C), the gas path opened. The gasification atmosphere at a flow of 0.7 m³/h was constituted by an air compressor and O₂, and its flow was controlled by a flowmeter and is represented by green color. In this experiment, the gas path of O₂ was closed as the gasification temperature was the main factor we considered. When the system had operated stably for 2 h, the fly ash was separated from the cyclone. Additionally, the gasification's fly ash was sieved to the size range of 0.106~0.83 mm. The product gas was cooled, filtered, dried, collected, and measured by a flue gas analyzer (MRU VARIO PLUS, Neckarsulm, Baden-Württemberg, Germany) to monitor the volume concentrations of H₂, CO, CO₂, and CH₄, represented by blue color. The operating conditions of all of the tests conducted are given in Table 3. The experiment used alumina as the bed material; its chemical composition is shown in Table 4.

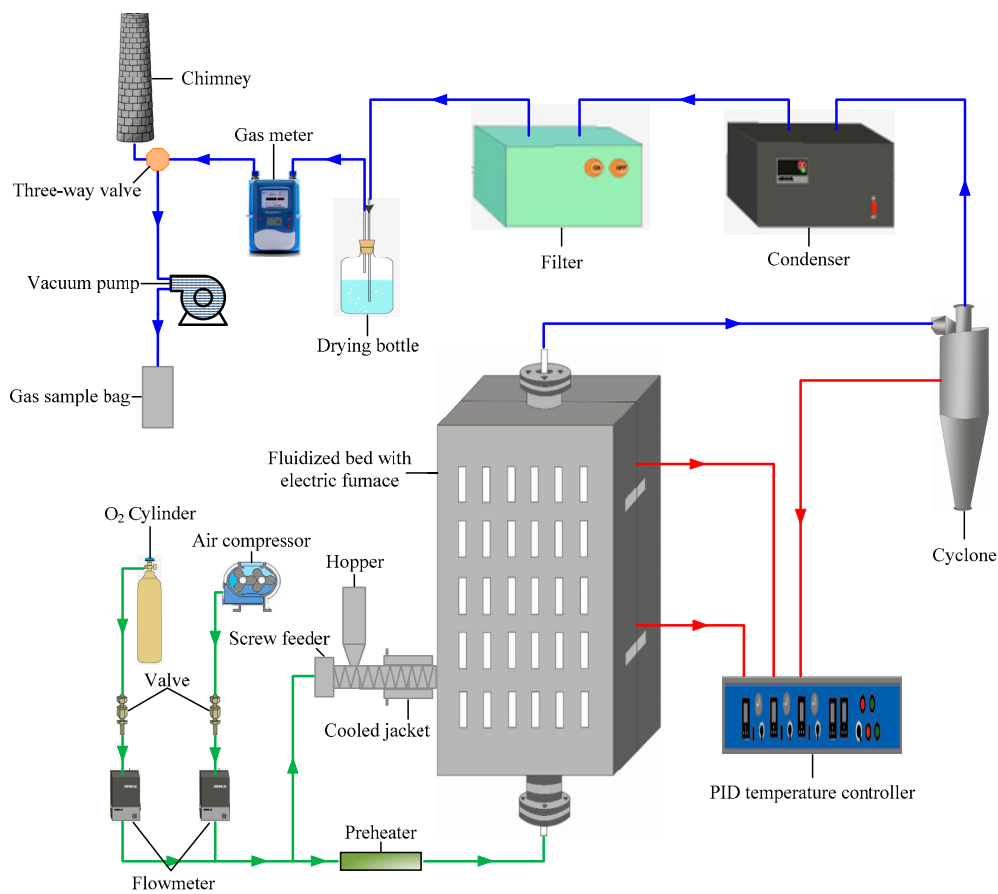


Figure 1. Biomass gasification fluidized bed experimental system. PID, Proportion-Integral-Derivative.

Table 3. Operating conditions.

Operating Parameter	Conditions	Units
Feeding rate of rice straw	1.11	kg/h
Bed temperature	600~800	°C
Superficial gas velocity ^a	0.7	m ³ /h
Bed material	alumina	–
Particle size of bed material	0.18~0.25	mm
Apparent density of bed material	2965	kg/m ³
Bulk density of bed material	1422	kg/m ³
Minimum fluidization velocity of bed material ^a	0.039	m/s

^a represents at 25 °C and 0.1 MPa.

Table 4. Bed material’s chemical properties.

Content	SiO ₂	Al ₂ O ₃	CaO	MgO	Fe ₂ O ₃	TiO ₂	K ₂ O	P ₂ O ₅	Others
%	14.18	79.41	0.32	0.02	2.41	3.29	0.09	0.22	0.06

2.3. Alkali Metal Measurement

The rice straw samples were firstly milled, then screened to obtain a diameter range from 0.08 to 0.109 mm [26], and dried at 100 °C for 2 h. Then, the samples were treated according to the following steps:

- 1 An accurately weighted 1 g of sample was dispersed in 250 mL of ultrapure water at room temperature while being stirred for 10 h. After filtration, leaching (more than three times),

and dilution, the dissolved sample was considered to contain the Water-Soluble form of alkali metal (WS), which was then detected by an induced coupled plasma emission spectrometer (ICP-AES) (Perkin Elmer, Boston, MA, USA).

- 2 The residual solid was dried and further dispersed in ammonium acetate (1 mol/L, 100 mL) under stirring for 5 h, and the mixture was repeatedly filtered and washed.
- 3 The residual solid was dispersed in hydrochloric acid (1 mol/L, 100 mL) under stirring for 5 h and then repeatedly filtered and washed. The washed solutions from the procedure in steps 2 and 3 were detected by ICP-AES as the Ammonium acetate-Soluble (AA) and Hydrochloric acid-Soluble (HA) forms of alkali metal, respectively.
- 4 At last, the last residual solid was dried at 105 °C for 24 h. The mixed-acid used for digestion was composed of 1 mL HF, 2.5 mL HCl, 5 mL HNO₃, and 0.3 mL H₂O₂. The residual solid and the reagent were sealed in Teflon ware containing digestion solution for 1 h. Then, 20 mL of saturated boric acid was added to the complex to an excess of F⁻ ion during the following digestion. The digestion solution was detected by ICP-AES to obtain the concentrations of Na and K in their Aluminosilicate Combination-Soluble (AC) forms. Data deviations were considered through five time measurements. All chemical wares made of glass and Teflon for the digestion procedures were immersed in 10% HNO₃ solution for at least 24 h and then rinsed with ultrapure water.

2.4. Characteristic Parameters of Gasification and Definition of Alkali Metal Release Rate

2.4.1. Calorific Value of Gas

The gas calorific value refers to the chemical energy contained in the gasification of combustible gas in the standard state. This research uses the low calorific value (*LHV*) of the latent heat of the vaporization of water vapor to measure the energy quality of the gasification. The *LHV* formula is:

$$LHV = 0.001 \times 4.2(30\varphi(\text{CO}) + 25.7\varphi(\text{H}_2) + 85.4\varphi(\text{CH}_4))(\text{MJ}/\text{m}^3). \quad (1)$$

In this equation, $\varphi(\text{H}_2)$, $\varphi(\text{CO})$, and $\varphi(\text{CH}_4)$, respectively, represent the volume percentage of the combustible gas of CO, H₂, and CH₄.

2.4.2. Gas Production Rate

The gas production rate refers to the volume of gas produced by the gasification of biomass raw materials in the standard state, which reflects the capacity of gas production. The definition is:

$$G_p = q_v / q_m. \quad (2)$$

In this equation, G_p , represents the gas production rate (m³/kg); q_v represents the volumetric flow rate of gas produced by gasification in standard conditions (m³/h); and q_m represents the biomass feeding rate (kg/h).

2.4.3. Gasification Efficiency

The gasification efficiency is the main index to measure the effect of gasification. It can be defined as the ratio of the combustible gas calorific value produced by the gasifier's gasification of the biomass raw materials and the calorific value within the raw material.

$$\eta = G_p \times \frac{LHV}{Q_{ar}} \times 100\% \quad (3)$$

In this equation, η represents the biomass gasification efficiency (%); and Q_{ar} represents the low calorific value received by the biomass raw materials (MJ/kg).

2.4.4. Carbon Conversion Rate

The carbon conversion rate is another main index to measure the effect of gasification. It is the ratio of the carbon content in the gas produced by the gasification of raw materials and the carbon content within the raw material.

$$\varphi_c = \frac{(\varphi(\text{CO}) + \varphi(\text{CO}_2) + \varphi(\text{CH}_4)) \times 12/22.4}{(100 - M_{ad}) \times C_{daf}/100} \times Y_g \times 100\% \quad (4)$$

In this equation, φ_c represents the carbon conversion rate (%); $\varphi(\text{CO}_2)$ represents the volume percentage of CO_2 ; and M_{ad} and C_{daf} are listed in Table 1.

2.4.5. Alkali Metal Release Rate

In this paper, because the content of ash in the rice straw is very low and the ash density is lower than the bed material, it was found that only a little ash remained in the slag. Therefore, the concentrations of Na and K were measured only in the fly ash. The relative release rates of Na and K were evaluated by Equation (1):

$$\eta_i = \frac{C_{0(i)} - C_{f(i)} \times C_a}{C_{0(i)}} \times 100\% \quad (5)$$

where $C_{0(i)}$ is the concentration of Na or K in the rice straw (mg/g); C_a is the ash yield of the gasification (mg/g); and $C_{f(i)}$ is the concentration of Na or K in the straw char under certain conditions (mg/g).

3. Results and Discussion

3.1. Effect of Gasification Temperature on Combustible Gas Composition

The effects of gasification temperature on gas composition and calorific value, gas yield, carbon conversion rate, and gasification efficiency are shown in Figure 2. Gasification temperature is a significant factor affecting volatile form and combustible gas composition [27–30]. As shown in Figure 2, with an increase in gasification temperature, the concentrations of CO and H_2 gradually increased in the gas produced, while the concentration of CO_2 significantly decreased and that of CH_4 slightly increased. The calorific value, gas yield, carbon conversion rate, and gasification efficiency increased gradually. This is because, in the biomass, cellulose, hemicellulose, and lignin tightly combine into a single organic material, similar to the glass fiber tissue in polymerized resin. During the gasification of the biomass, cellulose, hemicellulose, and lignin oxidised and decomposed, and the increase in the pyrolysis' reaction speed and the gasification's reforming reaction speed at a high temperature were the main reasons for the gas component change, which was shown as follows. First, the temperature accelerated the speed of the biomass's volatilization to split and the speed of the secondary cracking of the tar. It also improved the production of small molecule gases, such as H_2 , CO, and CH_4 [31,32]. Second, according to Le Chatelier's principle, the endothermic boudouard reaction and the water gas reaction were strengthened under a high temperature. More coke and CO_2 were converted to generate CO and H_2 , and the CO_2 concentration was further reduced. Third, the increasing temperature also promoted the reaction between H_2 and CO_2 to generate CO and H_2O , which caused an increase of CO concentration and a slight increase of H_2 concentration [33]. During the gasification process, cellulose, hemicellulose, and lignin oxidised and decomposed, and the increase of temperature and the quantity of the gasification reaction releases more free radicals, which is bound to affect the migration process of the alkali metal in rice straw.

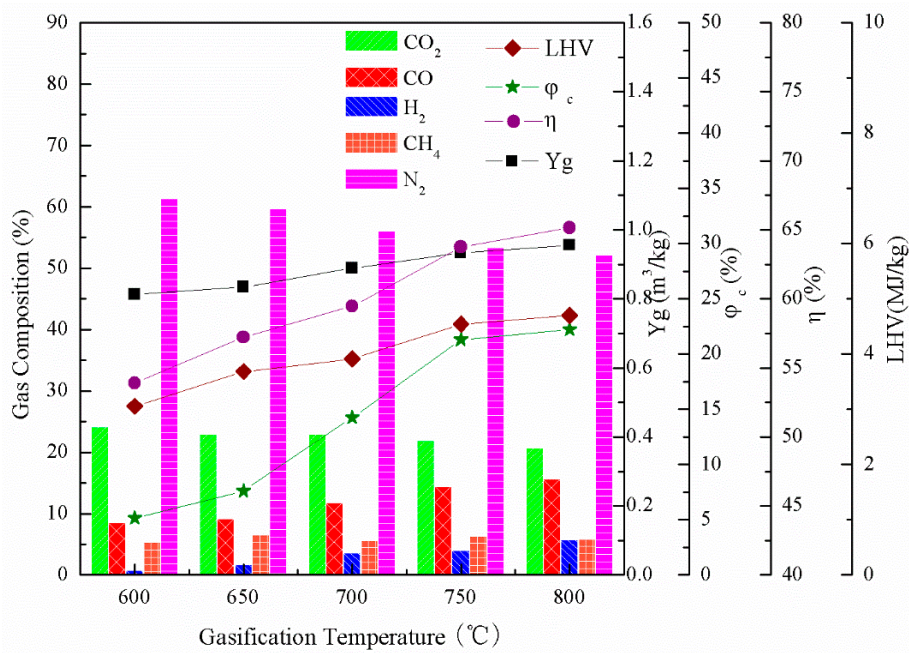


Figure 2. Effect of gasification temperature on combustible gas composition (air flow rate of 0.7 m³/h, biomass feed rate of 0.11 kg/h). LHV: low calorific value.

3.2. Analysis of the Occurrence Forms of Alkali Metals in Rice Straw

The contents of the occurrence forms of alkali metals in rice straw are shown in Table 5. The K concentration in the LTA was 83.86 mg/g, about 7 times as much as the 11.34 mg/g of Na concentration. For both Na and K, the concentrations in the LTA followed the decreasing sequence of WS > AA > HA > AC. The WS salts accounted for more than half of that (55.91% for Na and 69.64% for K), while the AC salts were the lowest (less than 5%), which is very different from coals, particularly for K. In coals, the insoluble K accounts for most of a sample: about 60.5–75.7% of total K [34]. This characteristic is closely related to the short growth period and the loose structure of rice straw; during the thermal treatment, the alkali metals easily evaporate during the thermal conversion process. The released Na and K may inhere on the surface of the char, form an activated center, and play a catalytic role during the gasification process.

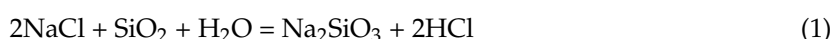
Table 5. Occurrence modes and contents of alkali metals in rice straw.

Alkali Metals	Water-Soluble	Ammonium Acetate-Soluble	Hydrochloric Acid-Soluble	Aluminosilicate Combination-Soluble	Total
Na (mg/g low-temperature ash)	6.34	3.33	1.14	0.53	11.34
Proportion of total Na (%)	55.91	29.35	10.07	4.65	100
K (mg/g low-temperature ash)	49.96	25.05	7.38	1.47	83.86
Proportion of total K (%)	69.64	20.73	7.87	1.76	100

3.3. Influence of Gasification Temperature on the Release Rate of Alkali Metals

The release rates of K and Na during gasification versus an increasing temperature are shown in Figure 3. The temperature on the release of Na is complicated. However, the release rate of Na is up to 50.2–70.8%, which means that the Na is easily released to its gas phase. Hirohataren has explained this phenomenon as Na reacting with Cl to form NaCl [35]. At 700–800 °C, with a temperature increase, the release rate of Na increases with non-linear growth. This may be because of the following. First, during the gasification process, that part of the Na which is released to its gas phase in the fuel gas is transferred to solid char. With a temperature increase, the mass transfer coefficient of gaseous Na to solid char increases, and makes the alkali metal transfer faster to solid char. Second, with a temperature increase,

the Na in the raw rice straw would be trapped and would interact with SiO_2 and Al_2O_3 in the bed material to form sodium aluminosilicates with low volatility according to the reactions (1) and (2) [34], which would result in the release rate of the Na in the gaseous phase being reduced. Third, the higher the temperature is, the more sufficient is the gasification conversion rate. Therefore, more Na adsorbed in the char can expose the surface to release it in its gaseous phase. Fourth, as shown in Table 1, the volatilization of rice straw is high (76.28%), so that with a temperature increase, a large amount of volatile material would be released quickly. So, a large number of free radicals would be released for thermal action. The free radicals released can react with the Na combined in the carbon substrate and improve the Na's evaporation to its gaseous phase. There is a competitive relationship between the factors 1, 2, 3 and 4. Therefore, the release rate of Na does not linearly increase with temperature.



The release rate reached the highest value of 70.8% at 750 °C. In this period, the evaporation of Na was faster than the conversion of non-volatile formation. However, when the temperature was higher than 750 °C, the release rate of Na decreased. It means that the conversion rate of non-volatile formation was much faster at 750 °C. Above all, the trend of the points appeared to be consistently increasing but nonlinear with gasification conversion. It can be deduced that temperature is not the only factor that impacts Na emission.

The release rate of K had an obvious step with the gasification temperature that was different from the high Na evaporation [35]. The release rate of K can be divided into two stages. The first stage is considered invariable below 700 °C, where the release rates of K range from 23.3% to 26.0%. The second stage was a sharp increase above 700 °C, where the releases rate of K increased up to 55.9%. A similar phenomenon was reported in Olsson's research as well, where the release rate of K increased linearly with an increasing gasification temperature from 700 to 800 °C [36].

From 600 to 800 °C, the release rates of Na were higher than those of K. The highest release rate of Na was 70.8% compared to that of K of only 55.9%. As shown in Table 5, compared with Na, the occurrence form of K was mostly a soluble inorganic salt and potassium ion, which was up to 69.64%, while little K was in an organic form. However, the release of inorganic K is much more difficult to produce than the release of its organic form in the gasification process, and in the experiment, the gasification temperature was not high enough for inorganic K to release. Besides that, the combination of K with C could cause a lower evaporation rate, while some compounds of Na, such as Na_2O and NaCl , are easier to evaporate [37–39].

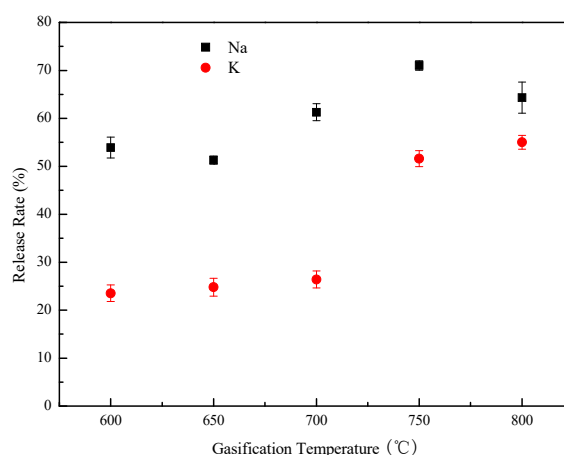


Figure 3. Variation of K and Na concentration in the gasification's ash.

3.4. Influence of Temperature on the Occurrence Form of the Alkali Metal

The influence of gasification temperature on the occurrence forms of Na and K are shown in Figures 4 and 5, respectively. The horizontal coordinate represents the gasification temperature, and the vertical coordinates represent the percent of total amount and the concentration of each occurrence form, respectively. Additionally, the detailed forms of Na and K are listed in Tables 6 and 7, respectively. From Tables 4–6, it can be seen that compared to LTA, there was a significant reduction of the concentration and proportion of the WS of Na in the fly ash with an increasing temperature, which was reduced from 6.34 mg/g and 55.9% to 2.1 mg/g and 39%, respectively. The amount of WS, AA and HA decreased with an increase of temperature, but not linearly. At a lower temperature, the Na released mainly in form of Na_3Cl_3 and Na_2Cl_2 . When the temperature was up to 800 °C, the Na released mainly as NaCl vapor [39]. The Na in the form of AC salts increased slightly with temperature, which is consistent with the research of Li, Zhang, and Song [34,40,41]. In addition to the Water-Soluble, Ammonium acetate-Soluble, and Hydrochloric acid-Soluble forms, an organic form also existed for Na in the fly ash. The reasons were proposed as follows. First, part of the Na combined with oxygen-containing functional groups and formed an intermediate substance O-Na+ group, which attached to the surface of char particles like pearls. The O-Na+ group is difficult to decompose due to the strong electron adsorption [16]. Second, part of the Na may also have combined with the char matrix to form a stable cross-linked structure [42,43]. These two forms of Na attach on the char stably, but there is no enough energy to break the keys to evaporate Na in this experiment. As a result, organic Na still existed in the fly ash.

Table 6. Occurrence modes and contents of Na ¹.

Gasification Temperature (°C)	WS (mg/g)	AA (mg/g)	HA (mg/g)	AC (mg/g)
600	1.91	1.44	1.18	0.63
650	2.10	1.48	1.35	0.71
700	1.64	1.21	0.82	0.70
750	1.23	0.94	0.49	0.65
800	1.49	0.96	0.62	0.84

¹ WS: Water-Soluble; AA: Ammonium acetate-Soluble; HA: Hydrochloric acid-Soluble; AC: Aluminosilicate Combination-Soluble.

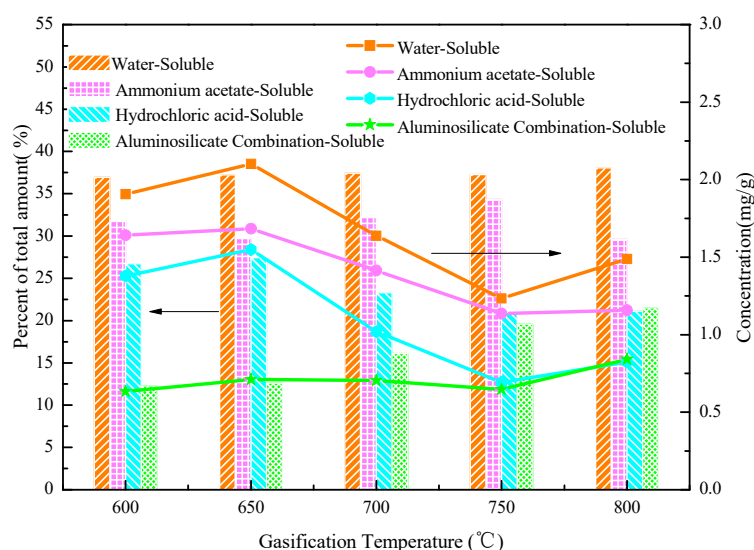


Figure 4. Variation of occurrence mode of Na with gasification temperature.

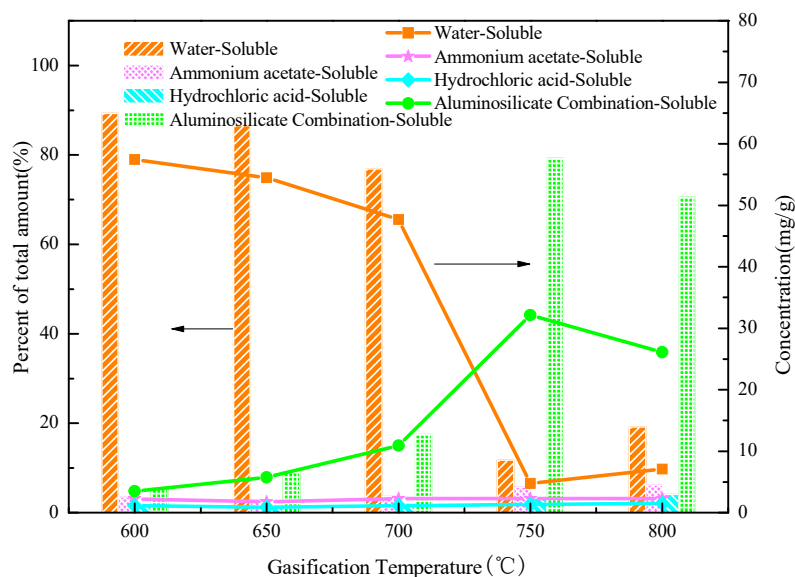


Figure 5. Variation of occurrence mode of K with gasification temperature.

Table 7. Occurrence modes and contents of K.

Gasification Temperature (°C)	WS (mg/g)	AA (mg/g)	HA (mg/g)	AC (mg/g)
600	57.44	2.26	1.14	3.49
650	54.47	1.75	0.91	5.77
700	47.71	2.28	1.14	10.93
750	4.77	2.29	1.33	32.12
800	7.09	2.29	1.51	26.09

Comparing Table 5 with Table 7 and Figure 5, the K in the form of silicate salts is difficult to react, and the concentration of the WS salts of K decreases from 69.642 to 55 mg/g, while that of the AA and HS forms of K both decrease to below 3 mg/g. It can be deduced that the K released before 700 °C was mainly in the form of organic salts of K. With the straw decomposing, the stronger evaporation of organic K was easy to evaporate due to its high thermal instability. It is generally considered that organic K begins to release at 200 °C with the release of volatile matter. When the temperature is higher than 700 °C, the concentration of K in the form of WS salts decreased from 69.642 mg/g and 20.733% to 7 mg/g and 20% compared with the LTA. In this period, the released K was in the form of water soluble inorganic salts that evaporated. Chen et al. used chemical thermodynamic equilibrium (FactSage) to calculate the evaporation temperature, and obtained that the inorganic K of biomass began to evaporate at 627 °C. The reactions of K with S, Si, Al, and so on produced salts with low volatility when the temperature was lower than 627 °C [4]. This is coincident with the result that the inorganic K that evaporated divided into two stages at the cut-off temperature of 700 °C. Yu et al. also obtained the result that the alkali metals that evaporated can be divided into two stages at the cut-off temperature of 500 °C [44]. So, the two stages of K release could be explained as follows: one path is organic K converted into its gaseous phase; the other path is soluble inorganic K volatilized at a high temperature. Specifically, with an increase in temperature, the number of AC salts of K increased. The possible reason is that the K reacted with the SiO₂, which accounts for 73.65% of fly ash, and produced a stable compound similar to K₂O·4SiO₂ [6,21,39,43,44]. So, the content of AC salts of K increased.

4. Conclusions

First, the contents of the four occurrence forms in rice straw followed the decreasing sequence of WS > AA > HA > AC. The content of WS accounted for more than 50%, while the content of AC was the lowest and was less than 5%. The first three occurrence forms were much easier to evaporate than the last one.

Second, the trend of the release rate of Na showed a consistent increase with gasification conversion, and the highest release rate reached 70.8%. However, the temperature was not the only factor to impact Na emission. The release of K can be divided into two stages with the cut-off temperature of 700 °C. The release rate of K increases sharply at 700 °C: up to 55.9%.

Third, the concentrations and the proportions of the WS, AA, and HA forms of Na in the fly ash decreased with an increase in temperature. The Na in the form of AC salts slightly increased with temperature. Organic Na was found as well.

Fourth, the concentration of WS salts of K decreased from 69.642 to 55 mg/g, and that of the AA and HA forms of K both decreased to 3 mg/g. The two release stages of K can be explained as follows: one path is organic K converted into its gaseous phase; the other path is soluble inorganic K volatilized at a high temperature. With an increase in temperature, the number of AC salts of K increased.

Acknowledgments: The financial support from the International S&T Cooperation Program of China (ISTCP, 2014DFE70150), the National Natural Science Foundation of China (No. 51476032 and No. 51706042), and the Fundamental Research Funds for the Central Universities (No. 2242016R20009) are greatly acknowledged.

Author Contributions: Tianyu Chen, Jun Cao and Baosheng Jin conceived and designed the experiments; Tianyu Chen performed the experiments; Tianyu Chen and Jun Cao analyzed the data; Tianyu Chen contributed reagents/materials/analysis tools; Tianyu Chen wrote the paper.

Conflicts of Interest: The authors declare no conflict of interest.

References

1. Heidenreich, S.; Foscolo, P.U. New concepts in biomass gasification. *Prog. Energy Combust. Sci.* **2015**, *46*, 72–95. [[CrossRef](#)]
2. Molino, A.; Chianese, S.; Musmarra, D. Biomass gasification technology: The state of the art overview. *J. Energy Chem.* **2016**, *25*, 10–25. [[CrossRef](#)]
3. Chianese, S.; Fail, S.; Binder, M.; Rauch, R.; Hofbauer, H.; Molino, A.; Blasi, A.; Musmarra, D. Experimental investigations of hydrogen production from CO catalytic conversion of tar rich syngas by biomass gasification. *Catal. Today* **2016**, *277*, 182–191. [[CrossRef](#)]
4. Chen, C.; Yu, C.J.; Zhang, H.L. Investigation on K and Cl release and migration in micro-spatial distribution during rice straw pyrolysis. *Fuel* **2016**, *167*, 180–187. [[CrossRef](#)]
5. Vassilev, S.V.; Baxter, D.; Andersen, L.K.; Vassileva, C.G. An overview of the chemical composition of biomass. *Fuel* **2010**, *89*, 913–933. [[CrossRef](#)]
6. Baxter, L.L.; Miles, T.R.; Miles, T.R., Jr.; Bryers, R.W.; Jenkins, B.M.; Milne, T.; Dayton, D.; Bryers, R.W.; Oden, L.L. The behavior of inorganic material in biomass-fired power boilers: Field and laboratory experiences. *Fuel Process. Technol.* **1998**, *54*, 47–80. [[CrossRef](#)]
7. Jensen, P.A.; Stenholm, M.; Hald, P. Deposition investigation in straw fired boilers. *Energy Fuels* **1997**, *11*, 1048–1055. [[CrossRef](#)]
8. Nielsen, H.P.; Larsen, O.H.; Frandsen, F.J.; Dam-Johansen, K. Deposition and high-temperature corrosion in a 10 MWth strawfired grate. *Fuel Process. Technol.* **1998**, *54*, 95–108.
9. Gilbe, C.; Ohman, M.; Lindstrom, E.; Bostrom, D.; Backman, R.; Samuelsson, R.; Burvall, J. Slagging characteristics during residential combustion of biomass pellets. *Energy Fuels* **2008**, *22*, 3536–3543. [[CrossRef](#)]
10. Knudsen, J.N.; Jensen, P.A.; Dam-Johansen, K. Transformation and release to the gas phase of Cl, K, and S during combustion of annual biomass. *Energy Fuels* **2004**, *18*, 1385–1399. [[CrossRef](#)]
11. Ohman, M.; Pommer, L.; Nordin, A. Bed agglomeration characteristics and mechanisms during gasification and combustion of biomass fuels. *Energy Fuels* **2005**, *19*, 1742–1748. [[CrossRef](#)]

12. Jiang, L.; Hu, S.; Xiang, J. Release characteristics of alkali and alkaline earth metallic species during biomass pyrolysis and steam gasification process. *Bioresour. Technol.* **2016**, *116*, 278–284.
13. Jensen, P.A.; Frandsen, F.J.; Dam-Johansen, K. Experimental investigation of the transformation and release to gas phase of potassium and chlorine during straw pyrolysis. *Energy Fuels* **2000**, *14*, 1280–1285. [[CrossRef](#)]
14. Saddawi, A.; Jone, J.M.; Williams, A. Influence of alkali metals on the kinetics of the thermal decomposition of biomass. *Fuel Process. Technol.* **2012**, *104*, 189–197. [[CrossRef](#)]
15. Dimple, M.Q.; Wu, H.W.; Hayashi, J. Volatilization and catalytic effects of alkali and alkaline earth metallic species during the pyrolysis and gasification of Victorian brown coal. Part IV. Catalytic effects of NaCl and ion-exchangeable Na in coal on char reactivity. *Fuel* **2003**, *82*, 587–593.
16. Wigmans, T.; Haringa, H. Nature, activity and stability of active sites during alkali metal carbonate-catalysed gasification reaction of coal char. *Fuel* **1983**, *62*, 185–189. [[CrossRef](#)]
17. Xu, S.Q.; Zhou, Z.J.; Dai, Z.G.; Yu, G.S.; Gong, X. Effects of alkalimetal and ash on crystallite structure of coal char during pyrolysis and on gasification reaction reactivity. *J. Chem. Eng. Chin. Univ.* **2010**, *24*, 64–70.
18. Bouraoui, Z.; Dupont, C.; Jeguirim, M.; Limousy, L.; Gadiou, R. CO₂ gasification of woody biomass chars: The influence of K and Si on char reactivity. *C. R. Chim.* **2016**, *19*, 457–465. [[CrossRef](#)]
19. Bouraoui, Z.; Jeguirim, M.; Guizani, C.; Limousy, L.; Dupont, C.; Gadiou, R. Thermogravimetric study on the influence of structural, textural and chemical properties of biomass chars on CO₂ gasification reactivity. *Energy* **2015**, *88*, 703–710. [[CrossRef](#)]
20. Joakim, M.; Johansen, M.A.; Kari, P.; Raili, T.; Helge, E.; Jon, G.J.; Flemming, J.F.; Peter, G. Release of K, Cl, and S during combustion and co-combustion with wood of high-chlorine biomass in bench and pilot scale fuel beds. *Proc. Combust. Inst.* **2013**, *34*, 2363–2372.
21. Keown, D.M.; Favas, G.; Hayashi, J.I.; Li, C.Z. Volatilisation of alkali and alkaline earth metallic species during the pyrolysis of biomass: Differences between sugar cane bagasse and cane trash. *Bioresour. Technol.* **2005**, *96*, 1570–1577. [[CrossRef](#)] [[PubMed](#)]
22. Pooya, L.; Zainal, A.Z.; Abdul, R.M.; Maedeh, M. CO₂ gasification reactivity of biomass char: Catalytic influence of alkali, alkaline earth and transition metal salts. *Bioresour. Technol.* **2013**, *144*, 288–295.
23. Narendra, S.; Sushil, A.; Mario, R.E.; Wang, Z.H.; Ryan, B. Southern pines char gasification with CO₂—Kinetics and effect of alkali and alkaline earth metals. *Fuel Process. Technol.* **2016**, *150*, 64–70.
24. Jeguirim, M.; Elmay, Y.; Limousy, L.; Lajili, M.; Said, R. Devolatilization behavior and pyrolysis kinetics of potential Tunisian biomass fuels. *Environ. Prog. Sustain.* **2014**, *33*, 1452–1458. [[CrossRef](#)]
25. Lv, D.Z.; Xu, M.H.; Liu, X.W.; Zhan, Z.; Li, Z.; Yao, H. Effect of cellulose, lignin, alkali and alkaline earth metallic species on biomass pyrolysis and gasification. *Fuel Process. Technol.* **2010**, *91*, 903–909. [[CrossRef](#)]
26. Musmarra, D. Influence of particle size and density on the jet penetration length in gas fluidized beds. *Ind. Eng. Chem. Res.* **2000**, *39*, 2612–2617. [[CrossRef](#)]
27. Gao, P.; Xue, L.; Lu, Q.; Dong, C. Effects of alkali and alkaline earth metals on N-containing species release during rice straw pyrolysis. *Energies* **2015**, *8*, 13021–13032. [[CrossRef](#)]
28. González-Vázquez, M.P.; García, R.; Pevida, C.; Rubiera, F. Optimization of a bubbling fluidized bed plant for low-temperature gasification of biomass. *Energies* **2017**, *10*, 306. [[CrossRef](#)]
29. James R., A.M.; Yuan, W.; Boyette, M.D. The effect of biomass physical properties on top-lit updraft gasification of woodchips. *Energies* **2016**, *9*, 283. [[CrossRef](#)]
30. Tamošiūnas, A.; Chouchène, A.; Valatkevičius, P.; Gimžauskaitė, D.; Aikas, M.; Uscila, R.; Ghorbel, M.; Jeguirim, M. The potential of thermal plasma gasification of olive pomace charcoal. *Energies* **2017**, *10*, 710. [[CrossRef](#)]
31. Liu, R.H.; Niu, W.S.; Zhang, D.L. *Biomass Thermochemical Conversion Technology*; Chem. Ind. Press: Oxford, UK, 2005; pp. 116–124.
32. Abu El-Rub, Z.; Bramer, E.A.; Brem, G. Experimental comparison of biomass chars with other catalysts for tar reduction. *Fuel* **2008**, *87*, 2243–2252. [[CrossRef](#)]
33. Moghadam, R.A.; Yusup, S.; Azlina, W.; Nehzati, S.; Tavasoli, A. Investigation on syngas production via biomass conversion through the integration of pyrolysis and air-steam gasification processes. *Energy Convers. Manag.* **2014**, *87*, 670–675. [[CrossRef](#)]
34. Song, G.; Yang, S.; Song, W.; Qi, X. Release and transformation behaviors of sodium during combustion of high alkali residual carbon. *Appl. Therm. Eng.* **2017**, *122*, 285–296. [[CrossRef](#)]

35. Hirohata, O.; Wakabayashi, T.; Tasska, K.; Fushimi, C.; Furusawa, T.; Kuchonthara, P.; Tsutsumi, A. Release behavior of tar and alkali and alkaline earth metals during biomass steam gasification. *Energy Fuels* **2008**, *22*, 4235–4239. [[CrossRef](#)]
36. Olsson, J.G.; Pettersson, J.B.C.; Padban, N.; Bjerle, I. Alkali metal emission from filter ash and fluidized bed material from PFB gasification of biomass. *Energy Fuels* **1998**, *12*, 626–630. [[CrossRef](#)]
37. Werkelin, J.; Skrifvars, B.J.; Zevenhoven, M.; Holmbom, B.; Hupa, M. Chemical forms of ash-forming elements in woody biomass fuels. *Fuel* **2010**, *89*, 481–493. [[CrossRef](#)]
38. Dong, K. *The Migration Patterns of Chlorine and Alkali Metals (K and Na) in the Biomass Combustion*; Harbin Institute of Technology: Harbin, China, 2011.
39. Han, X.; Zhang, Y.F.; Yao, D.D.; Qian, K.Z.; Yang, H.P.; Wang, X.H. Releasing behavior of alkali and alkaline earth metals during biomass gasification. *J. Fuel Chem. Technol.* **2014**, *42*, 792–798.
40. Li, G.; Wang, C.A.; Yan, Y.; Jin, X.; Liu, Y.; Che, D. Release and transformation of sodium during combustion of Zhundong coals. *J. Energy Inst.* **2016**, *89*, 48–56. [[CrossRef](#)]
41. Zhang, J.; Han, C.L.; Yan, Z.; Liu, K.; Xu, Y.; Sheng, C.D.; Pan, W.P. The varying characterization of Alkali Metals (Na, K) from coal during the initial stage of coal combustion. *Energy Fuels* **2001**, *15*, 2957–2960. [[CrossRef](#)]
42. Sathe, C.; Pang, Y.Y.; Li, C.Z. Effects of heating rate and ion-exchange cations on the pyrolysis yields from a Victorian brown coal. *Energy Fuels* **1999**, *13*, 748–755. [[CrossRef](#)]
43. Quyn, D.M.; Hayashi, J.I.; Li, C. Volatilisation of alkali and alkaline earth metallic species during the gasification of a Victorian brown coal in CO₂. *Fuel Process. Technol.* **2005**, *86*, 1241–1251. [[CrossRef](#)]
44. Yu, C.J.; Tang, Y.L.; Feng, M.X.; Luo, Z.Y.; Ceng, K. Experimental study on alkali emission during rice straw pyrolysis. *J. Zhejiang Univ. Sci.* **2005**, *39*, 1435–1438.



© 2017 by the authors. Licensee MDPI, Basel, Switzerland. This article is an open access article distributed under the terms and conditions of the Creative Commons Attribution (CC BY) license (<http://creativecommons.org/licenses/by/4.0/>).